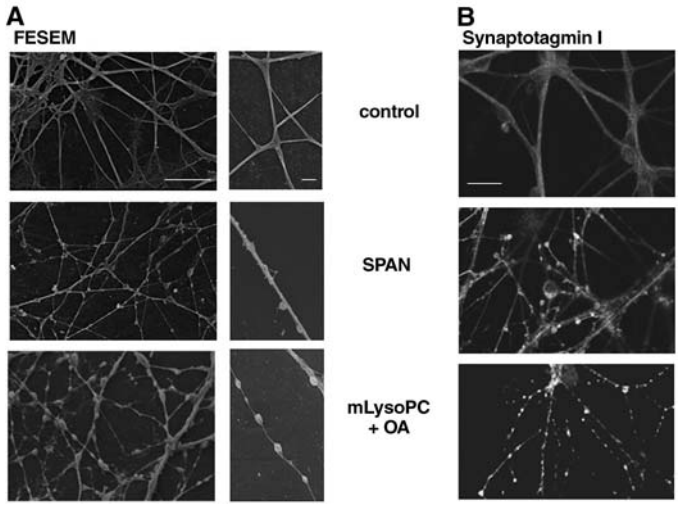


**Fig. 2.** Field emission scanning electron microscopy (FESEM) of cerebellar granular neurons exposed to taipoxin (6 nM for 60 min) or mLysoPC+OA (30 μM for 15 min) at lower (left panels) and higher (right panels) magnifications (**A**). Identical results were obtained with notexin, β-bungarotoxin, and textilotoxin. Scale bar, 10 μm (left panels) and 2 μm (right panels). (**B**) Cerebellar neurons were exposed to 6 nM β-bungarotoxin for 60 min or to 30 μM mLysoPC+OA for 15 min and stained with an antibody specific for the lumenal domain of synaptotagmin I before fixation. Samples were processed for indirect immunofluorescence without permeabilization; superimposable results were obtained with notexin, taipoxin, and textilotoxin in cerebellar neurons and hippocampal neurons. Scale bar, 10 μm.

ment of PLA2 in other exocytotic events such as the sperm acrosomal exocytosis (*24*). Furthermore, a SPAN microinjected into pheochromocytoma cells inhibited neuroexocytosis (*25*), presumably because it acted on the cytosolic plasma membrane side, inducing an opposite membrane configuration. The presence of clathrin-coated Ω-shaped structures in SPAN-poisoned NMJs (*4*–*7*) suggested that they also inhibit synaptic vesicle fission from the plasma membrane (*3*, *14*). Indeed, the same SPAN-induced lipid changes promoting membrane fusion do inhibit membrane fission for the same physical and topological reasons (*17*).

### References and Notes

1. R. M. Kini, Ed., *Venom Phospholipase A2 Enzymes* (Wiley, Chichester, UK, 1997).
2. G. Schiavo, M. Matteoli, C. Montecucco, *Physiol. Rev.* **80**, 717 (2000).
3. C. Montecucco, O. Rossetto, *Trends Biochem. Sci.* **25**, 266 (2000).
4. S. G. Cull-Candy, J. Fohlman, D. Gustavsson, R. Lullmann-Rauch, S. Thesleff, *Neuroscience* **1**, 175 (1976).
5. I. L. Chen, C. Y. Lee, *Virchows Arch. B Cell Pathol.* **6**, 318 (1970).
6. J. B. Harris, B. D. Grubb, C. A. Maltin, R. Dixon, *Exp. Neurol.* **161**, 517 (2000).
7. C. Y. Lee, M. C. Tsa, Y. M. Chen, A. Ritonja, F. Gubensek, *Arch. Int. Pharmacodyn. Ther.* **268**, 313 (1984).
8. P. Rosenberg, *Venom Phospholipase A2 Enzymes*, R. M. Kini, Ed. (Wiley, Chichester, UK, 1997), pp. 155-183.
9. R. M. Kini, *Toxicon* **42**, 827 (2003).
10. C. C. Yang, in *Venom Phospholipase A2 Enzymes*, R. M. Kini, Ed. (Wiley, Chichester, UK,1997), pp. 185-204.
11. R. E. Stafford, T. Fanni, E. A. Dennis, *Biochemistry* **28**, 5113 (1989).
12. J. Wang *et al.*, *Br. J. Pharmacol.* **141**, 586 (2004).
13. M. Rigoni *et al.*, *J. Cell Sci.* **15**, 3561 (2004).
14. D. Bonanomi *et al.*, *Mol. Pharmacol.* **67**, 1901 (2005).
15. F. Kamp, D. Zakim, F. Zhang, N. Noy, J. A. Hamilton, *Biochemistry* **34**, 11928 (1995).
16. L. V. Chernomordik, E. Leikina, V. Frolov, P. Bronk, J. Zimmerberg, *J. Cell Biol.* **136**, 81 (1997).
17. L. V. Chernomordik, M. M. Kozlov, *Annu. Rev. Biochem.* **72**, 175 (2003).
18. Y. Xu, F. Zhang, Z. Su, J. A. McNew, Y. K. Shin, *Nat. Struct. Mol. Biol.* **12**, 417 (2005).
19. C. G. Giraudo *et al.*, *J. Cell Biol.* **170**, 249 (2005).
20. C. Reese, F. Heise, A. Mayer, *Nature* **436**, 410 (2005).
21. K. Farsad, P. De Camilli, *Curr. Opin. Cell Biol.* **15**, 372 (2003).
22. R. Jahn, T. Lang, T. C. Sudhof, *Cell* **112**, 519 (2003).
23. L. K. Tamm, J. Crane, V. Kiessling, *Curr. Opin. Struct. Biol.* **13**, 453 (2003).
24. E. R. S. Roldan, *Front. Biosci.* **3**, 1119 (1998).
25. S. Wei *et al.*, *Neuroscience* **121**, 891 (2003).
26. Supported by Telethon grant GP0272Y01, COFIN Project 2002055747, FISR-DM 16/10/00, FIRB-RBNE01RHZM, University of Padova, and Cancer Research UK.

**Supporting Online Material**

www.sciencemag.org/cgi/content/full/310/5754/1678/DC1
Materials and Methods
Figs. S1 and S2
References

27 September 2005; accepted 4 November 2005
10.1126/science.1120640

# Neural Systems Responding to Degrees of Uncertainty in Human Decision-Making

**Ming Hsu,[1] Meghana Bhatt,[1] Ralph Adolphs,[1,2] Daniel Tranel,[2] Colin F. Camerer[1]***

**Much is known about how people make decisions under varying levels of probability (risk). Less is known about the neural basis of decision-making when probabilities are uncertain because of missing information (ambiguity). In decision theory, ambiguity about probabilities should not affect choices. Using functional brain imaging, we show that the level of ambiguity in choices correlates positively with activation in the amygdala and orbitofrontal cortex, and negatively with a striatal system. Moreover, striatal activity correlates positively with expected reward. Neurological subjects with orbitofrontal lesions were insensitive to the level of ambiguity and risk in behavioral choices. These data suggest a general neural circuit responding to degrees of uncertainty, contrary to decision theory.**

In theories of choice under uncertainty used in social sciences and behavioral ecology, the only variables that should influence an uncertain choice are the judged probabilities of possible outcomes and the evaluation of those outcomes. But confidence in judged probability can vary widely. In some choices, such as gambling on a roulette wheel, probability can be confidently judged from relative frequencies, event histories, or an accepted theory. At the other extreme, such as the chance of a terrorist attack, probabilities are based on meager or conflicting evidence, where important information is clearly missing. The two types of uncertain events are often called risky and ambiguous, respectively. In subjective expected utility theory, the probabilities of outcomes should influence choices, whereas confidence about those probabilities should not. But experiments show that many people are more willing to bet on risky outcomes than on ambiguous ones, holding judged probability of outcomes constant (*1*). This empirical aversion to ambiguity motivates a search for neural distinctions between risk and ambiguity. Here, we extend the study of the neural basis of decision under risk to encompass ambiguity.

The difference between risky and ambiguous uncertainty is illustrated by the Ellsberg paradox (*2*). Imagine one deck of 20 cards composed of 10 red and 10 blue cards (the risky deck). Another deck has 20 red or blue cards, but the composition of red and blue cards is completely unknown (the ambiguous deck). A bet on a color pays a fixed sum (e.g., $10) if a card with the chosen color is drawn, and zero otherwise (Fig. 1A).

[1]Division of Humanities and Social Sciences, 228-77, California Institute of Technology, Pasadena, CA 91125, USA. [2]University of Iowa Medical School, Iowa City, IA 52242, USA.

*To whom correspondence should be addressed. E-mail: camerer@hss.caltech.edu

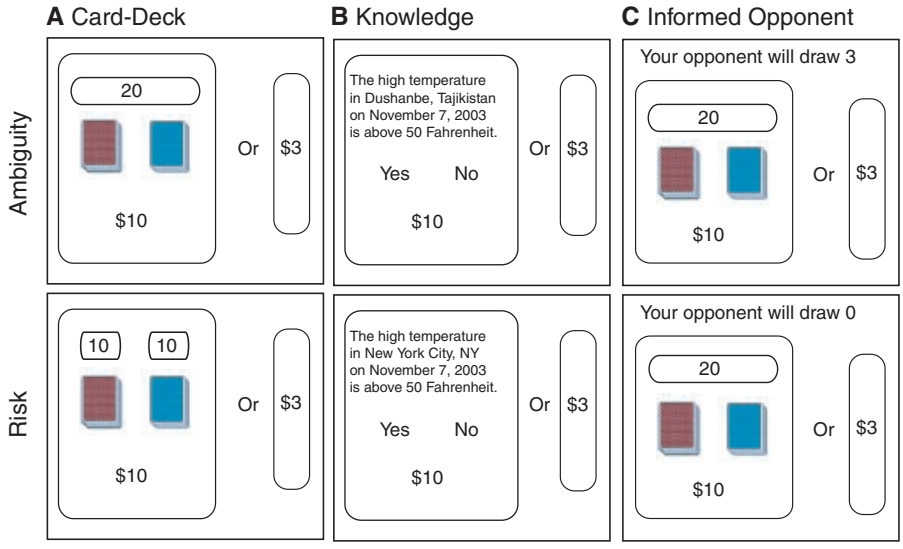


**Fig. 1.** Sample screens from the experiment. The conditions in the top panel are called ambiguous because the subject is missing relevant information that is available in the risk conditions (bottom panel). Subjects always choose between betting on one of the two options on the left side or taking the certain payoff on the right. (**A**) Card-Deck treatment: Ambiguity is not knowing the exact proportion; risk is knowing the number of cards (indicated by numbers above each deck). (**B**) Knowledge treatment: Ambiguity is knowing less about the uncertain events (e.g., Tajikistan) relative to risk (e.g., New York City). (**C**) Informed Opponent treatment: Ambiguity is betting against an opponent who has more information (who drew a three-card sample from the deck) than in risk (where the opponent drew no cards from the deck). Bets win if subject chooses the realized color and opponent chooses the opposite color; otherwise, both take the certain payoff [see (*17*)].

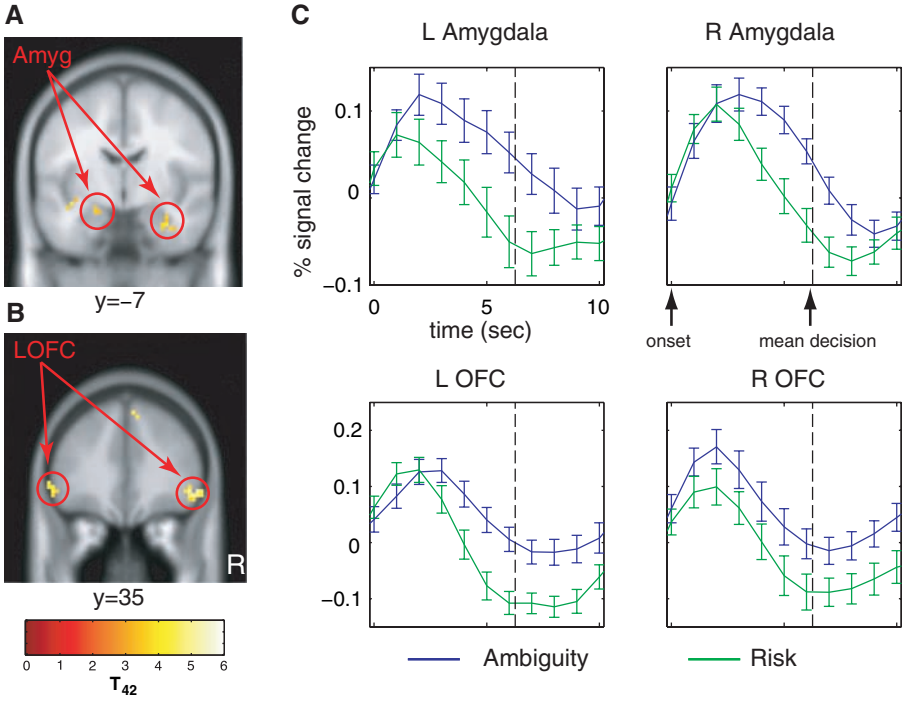


**Fig. 2.** Regions showing greater activation in response to ambiguity than in response to risk. Random-effects analysis of all three treatments revealed regions that are differentially activated in decision-making under ambiguity relative to risk ($P \leq 0.001$, uncorrected; cluster size $k \geq 10$ voxels). These regions include (**A**) left amygdala and right amygdala/parahippocampal gyrus (coronal section shown at $y = 7$ in MNI space; heat map represents $t$ statistic with 42 degrees of freedom) and (**B**) bilateral OFC. (**C**) Mean time courses of amygdala and OFC (time synched to trial onset, dashed vertical lines are mean decision times; error bars are SEM; $n = 16$).

In experiments with these choices, many would rather bet on a red draw from the risky deck than on a red draw from the ambiguous deck, and similarly for blue (*3*, *4*). If betting preferences are determined only by probabilities and associated payoffs, this pattern is a paradox. In theory, disliking the bet on a red draw from the ambiguous deck implies that its subjective probability is lower [$P_{amb}$(red) < $P_{risk}$(red)]. The same aversion for the blue bets implies $P_{amb}$(blue) < $P_{risk}$(blue). But these inequalities, and the fact that the probabilities of red and blue must sum to 1 for each deck, imply $1 = P_{amb}(\text{red}) + P_{amb}(\text{blue}) < P_{risk}(\text{red}) + P_{risk}(\text{blue}) = 1$, a contradiction. The paradox can be resolved by allowing choices to depend both on subjective probabilities of events and on the ambiguity of those events (*5*–*7*). More generally, choices can depend on how much relevant information is missing or how ignorant people feel compared to others (*8*, *9*).

We explored the neural differences with varying levels of uncertainty by using a combination of data from functional magnetic resonance imaging (fMRI) and behavioral data from lesion patients. This study builds on previous findings in neuroscience on reward and uncertainty. In particular, we focus on the striatum, which has been implicated in reward anticipation (*10*); the orbitofrontal cortex (OFC), where patients with lesions perform poorly on behavioral tasks involving uncertainty, such as the Iowa gambling task (*11*); and the amygdala, which responds to ambiguous facial cues and has been hypothesized as a generalized vigilance module in the brain (*12*–*14*).

The fMRI study used three experimental treatments: The Card-Deck treatment is a baseline pitting pure risk (where probabilities are known with certainty) against pure ambiguity. The Knowledge treatment uses choices about events and facts, which fall along a spectrum from risk to ambiguity. In the Informed Opponent treatment, the subject bets against another person who has seen a sample of cards from the deck. This opponent is therefore better informed about the contents of the ambiguous deck (*15*). This condition corresponds to a commonly posited theory of ambiguity aversion: Even when there is no informed opponent, people act as if there is (*16*). All three treatments have one condition where the subject is missing information (ambiguity) relative to the other condition (risk).

Subjects made 48 choices in each treatment between certain amounts of money and bets on card decks or events (*17*). The amounts of the certain payoff and the bet payoff varied across trials. In the Card-Deck and Informed Opponent treatments, the number and proportions of cards also varied. We estimated a general linear model (GLM) using standard regression techniques (*17*). Two primary regressors were used for each treatment—one for ambiguity trials and one for risky trials—beginning at the onset of the stimulus and ending at the time of decision. To find regions differentially activated by ambiguity and risk, we performed a random-effects analysis pooling all three treatments, correcting for nonsphericity (*17*).

Regions that were more active during the ambiguous condition relative to the risk condi-

tion included the OFC and amygdala (Fig. 2A) and the dorsomedial prefrontal cortex (DMPFC) (fig. S8 and table S7). These areas have been implicated in integration of emotional and cognitive input (OFC) (*18*), reaction to emotional information (amygdala) (*19*–*21*), and modulation of amygdala activity (DMPFC) (*12*). Areas activated during the risk condition relative to ambiguity include the dorsal striatum (caudate nucleus) (Fig. 3A). Furthermore, the dorsal striatal activations were also correlated with the expected value of actual choices (Fig. 3C), whereas no such correlation was observed in the OFC or amygdala (tables S11 and S12). This, together with other studies implicating the dorsal striatum in reward prediction (*10*, *22*–*24*), supports the hypothesis that ambiguity lowers the anticipated reward of decisions.

Time courses showed different patterns of activation in the ambiguity > risk and risk > ambiguity regions. Whereas the amygdala and OFC reacted rapidly at the onset of the trial (Fig. 2C), the dorsal striatum activity built more slowly (Fig. 3B) (fig. S4) and peaked significantly later (fig. S7) than those of the amygdala and OFC. This difference was present in all three experimental treatments (figs. S3 and S4) and appeared to be independent of subjects' choices (fig. S6) (*25*). The temporal difference between these ambiguity and risk regions is consistent with the presence of two interacting systems—a "vigilance"/evaluation system in the amygdala (*26*) and OFC, which responds more rapidly to the stimuli and grades uncertainty, and a reward-anticipation system in the striatum that is further downstream.

Parameters measuring ambiguity and risk aversion (γ and ρ, respectively) were estimated from a nonlinear stochastic model of the subjects' choice behavior in our tasks (*27*). Ambiguity aversion, measured by γ, was positively correlated with contrast values between ambiguity and risk (averaged over the three treatments) in the right OFC ($r = 0.55$, $P < 0.04$, two-tailed) and more weakly in the left OFC ($r = 0.37$, $P < 0.2$, two-tailed) (*17*).

To validate the fMRI results and establish that the OFC plays a necessary role in distinguishing levels of uncertainty, we conducted behavioral experiments similar to the card-deck task above, using a lesion method (*17*). Twelve neurological subjects with focal brain lesions were partitioned into two groups: those whose lesions included the most significant activation focus in the OFC revealed in our fMRI study ($n = 5$), and a comparison group (temporal lobe damage patients) whose lesions did not overlap with any of our fMRI foci ($n = 7$). The two groups had similar etiology, IQ, mathematical ability, and performance on other background tasks (table S15).

Two-dimensional confidence interval analysis (Fig. 4) showed that frontal patients are risk- and ambiguity-neutral (i.e., the hypothesis that $\gamma = \rho = 1$ cannot be rejected). This differed from the comparison group, who appeared to be risk- and ambiguity-averse. The OFC-lesioned group therefore did not distinguish between degrees of uncertainty (ambiguity and risk). This is behaviorally abnormal but is consistent, ironically, with the logic of subjective expected utility theory.

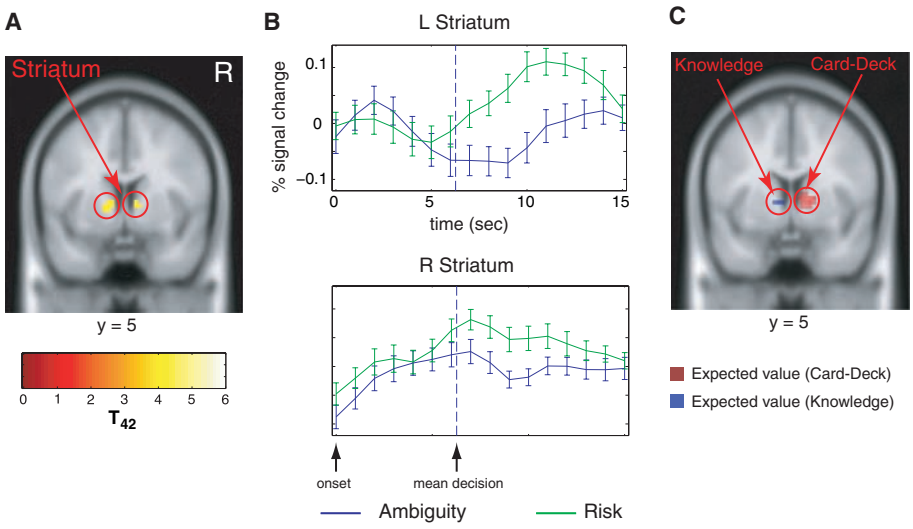


**Fig. 3.** Regions showing greater activation in response to risk than in response to ambiguity. Random-effects analysis of all three treatments revealed brain regions that are differentially activated in decision-making under risk. These regions include (**A**) dorsal striatum, as well as precuneus and premotor cortex (table S8) ($P \leq 0.001$, uncorrected; cluster size $k \geq 10$ voxels.) (**B**) Mean time courses for risk regions (time synched to trial onset, dashed vertical lines are mean decision times; error bars are SEM; $n = 16$). (**C**) Regions of the dorsal striatum significantly correlated with expected values of subjects' choices in risk condition of Card-Deck treatment (red) and both risk and ambiguity conditions of Knowledge treatment (blue) ($P < 0.005$, uncorrected; cluster size $k \geq 10$ voxels).

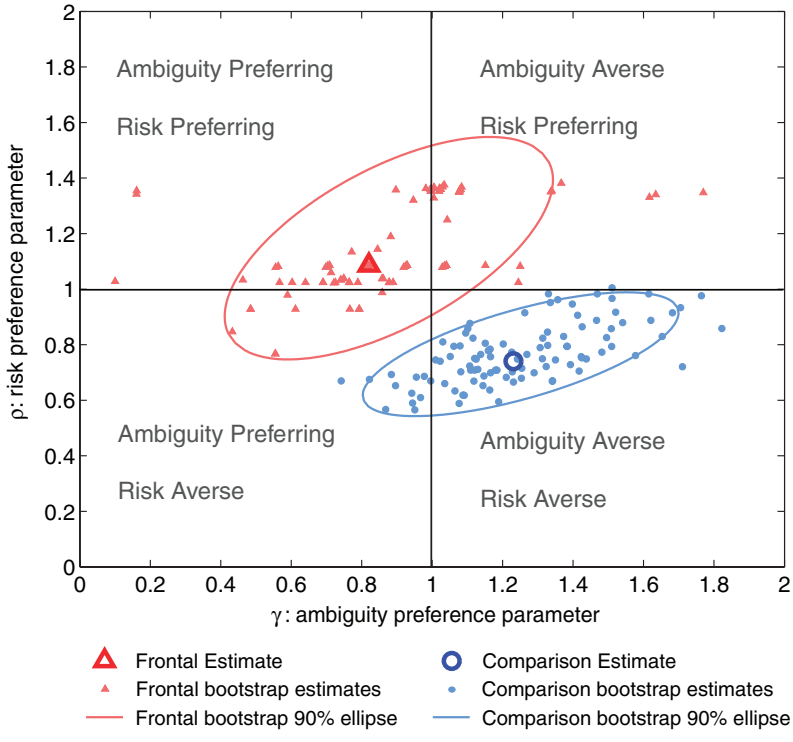


**Fig. 4.** Risk and ambiguity attitudes of OFC patients ($n = 5$) and lesion comparisons ($n = 7$) with associated 90% confidence intervals. The risk neutral line ($\rho = 1$) and the ambiguity neutral line ($\gamma = 1$) demarcate four quadrants as labeled. Open symbols plot maximum likelihood estimates of a group-level stochastic choice model. Frontals: ($\gamma = 0.82$, $\rho = 1.09$); lesion comparisons: ($\gamma = 1.23$, $\rho = 0.74$) [see (*17*)]. Solid symbols represent 100 bootstrapped ($\gamma$, $\rho$) estimates. Ellipses are two-dimensional 90% confidence intervals around the bootstrapped data. Angle of the ellipse reflects correlation between ρ and γ (0.42 for frontal, 0.31 for comparison).

Together with the fMRI results, these data suggest a neural system for evaluating general uncertainty. Both the amygdala and OFC are known to receive rapid, multimodal sensory input; both are bidirectionally connected and are known to function together in evaluating the value of stimuli (*28*); and both are likely involved in detecting salient and relevant stimuli of uncertain value. The latter function has been hypothesized especially for the amygdala (*26*, *29*). Such a function also provides a reward-related signal that can motivate behavior, by virtue of the known connections between the amygdala/OFC and the striatum (*30*). Although the circuit is assessed here in the context of a neuroeconomic experiment, we believe that it subserves general aspects of how organisms explore their environment: Under uncertainty, the brain is alerted to the fact that information is missing, that choices based on the information available therefore carry more unknown (and potentially dangerous) consequences, and that cognitive and behavioral resources must be mobilized in order to seek out additional information from the environment.

Understanding the neural basis of choice under uncertainty is important because it is a fundamental activity at every societal level, with examples as diverse as people saving for retirement, companies pricing insurance, and countries evaluating military, social, and environmental risks (*17*). The choices can vary greatly in the level of information available to the decision-maker about outcome probabilities. Standard decision theory, however, precludes agents from acting differently in the face of risk and ambiguity. Our results show that this hypothesis is wrong on both the behavioral and neural level, and suggest a unified treatment of ambiguity and risk as limiting cases of a general system evaluating uncertainty. For neuroscientists, these results introduce the important concept of varying degrees of uncertainty that is missing from previous studies of reward and decision-making. More generally, this study shows the value of combining ideas and tools from social and biological sciences (*31*, *32*).


**References and Notes**

1. C. Camerer, M. Weber, *J. Risk Uncert.* **5**, 325 (1992).
2. D. Ellsberg, *Q. J. Econ.* **75**, 643 (1961).
3. S. Becker, F. Brownson, *J. Polit. Econ.* **72**, 62 (1964).
4. K. MacCrimmon, *Risk and Uncertainty*, K. Borch, J. Mossin, Eds. (Macmillan, London, 1968).
5. If ambiguous probabilities are subadditive, then $1 - P_{amb}(\text{red}) - P_{amb}(\text{blue})$ represents reserved belief and indexes the degree of aversion to ambiguity. Some models assume that probabilities are additive but are set-valued, and assume that the worst probability in the set determines their chances (*6*, *7*). This model and others are silent about possible neural circuitry.
6. D. Schmeidler, *Econometrica* **57**, 571 (1989).
7. I. Gilboa, D. Schmeidler, *J. Math. Econ.* **18**, 141 (1989).
8. D. Frisch, J. Baron, *J. Behav. Decision Making* **1**, 149 (1988).
9. C. Fox, A. Tversky, *Q. J. Econ.* **110**, 585 (1995).
10. W. Schultz, *Nat. Rev. Neurosci.* **1**, 199 (2000).
11. A. Bechara, D. Tranel, H. Damasio, *Brain* **123**, 2189 (2000).
12. H. Kim *et al.*, *J. Cogn. Neurosci.* **16**, 1730 (2004).
13. H. Kim, L. H. Somerville, T. Johnstone, A. L. Alexander, P. J. Whalen, *Neuroreport* **14**, 2317 (2003).
14. E. Phelps *et al.*, *J. Cogn. Neurosci.* **12**, 729 (2000).
15. The Informed Opponent treatment is as follows: (i) Both subjects choose a color, with the opponent having sampled the specified number of cards from the ambiguous deck; (ii) a card is chosen from the deck; and (iii) the person with the color that matches that of the card chosen wins the bet. Mismatches make nothing (*17*). The Informed Opponent hypothesis is that bets on ambiguous card decks and low-knowledge events, although normatively different from bets against the informed opponent, are generated by similar neural circuitry. Similarity of time courses in the amygdala, OFC, and striatum across all three treatments (figs. S3 and S4) is consistent with this hypothesis.
16. A. Kühberger, J. Perner, *J. Behav. Decision Making* **16**, 181 (2003).
17. See supporting data on *Science* Online.
18. H. Critchley, C. Mathias, R. Dolan, *Neuron* **29**, 537 (2001).
19. A. Bechara, H. Damasio, A. Damasio, *Ann. N.Y. Acad. Sci.* **985**, 356 (2003).
20. R. Adolphs, *Curr. Opin. Neurobiol.* **12**, 169 (2002).
21. H. Critchley, R. Elliot, C. Mathias, R. Dolan, *J. Neurosci.* **20**, 3033 (2000).
22. J. O'Doherty *et al.*, *Science* **304**, 452 (2004).
23. B. Knutson, C. Adams, G. Fong, D. Hommer, *J. Neurosci.* **21**, RC159 (2001).
24. One earlier positron emission tomography study (*33*) also found differential activation in the caudate during risk relative to ambiguity (www.econ.umn.edu/~arust/C-CAll.pdf, p6).
25. The areas that are differentially activated by the choice that subjects make (gamble or certain payoff) include the caudate head and the insula (table S9), which are also not significantly interacting with ambiguity/risk.
26. P. J. Whalen, *Curr. Direct. Psychol. Sci.* **7**, 177 (1998).
27. Aversion to risk is measured by the concavity of the subjective utility function for money, $u(x) = x^{\rho}$. Lower $\rho$ corresponds to more risk aversion. Aversion to ambiguity (controlling for risk aversion) is measured by the degree to which probabilities $P$ are underweighted when they are ambiguous, $w(P) = P^{\gamma}$. Higher $\gamma$ corresponds to more ambiguity aversion. Best fitting values of $\rho$ and $\gamma$ are estimated via maximum likelihood (*17*).
28. D. Gaffan, E. A. Murray, M. Fabre-Thorpe, *Eur. J. Neurosci.* **5**, 968 (1993).
29. R. B. Adams Jr., H. L. Gordon, A. A. Baird, N. Ambady, R. E. Kleck, *Science* **300**, 1536 (2003).
30. D. Amaral, J. Price, A. Pitkanen, S. Carmichael, in *The Amygdala: Neurobiological Aspects of Emotion, Memory, and Mental Dysfunction*, J. P. Aggleton, Ed. (Wiley, New York, 1992), pp. 1–66.
31. P. Glimcher, A. Rustichini, *Science* **306**, 447 (2004).
32. S. M. McClure, D. Laibson, G. Loewenstein, J. D. Cohen, *Science* **306**, 503 (2004).
33. A. Rustichini, J. Dickhaut, P. Ghiradato, K. Smith, J. Pardo, *Games Econ. Behav.* **52**, 257 (2005).



34. We thank K. Scheer and M. Koenigs for data collection, and P. Bossaerts and S. Quartz for valuable input in the planning stages of this work. Supported by NSF grant SES 0433010 (C.C. and R.A.), the MacArthur Foundation Preferences Network (C.C.), Caltech grant CFC.PROVOST-3-GRANT (C.C.), NIH grants R01 MH067681 (R.A.) and P01 NS19632 (D.T.), and the David and Lucile Packard Foundation.


**Supporting Online Material**

www.sciencemag.org/cgi/content/full/310/5754/1680/DC1
Materials and Methods
Figs. S1 to S8
Tables S1 to S15
References


26 May 2005; accepted 20 October 2005
10.1126/science.1115327


# A Conserved Checkpoint Monitors Meiotic Chromosome Synapsis in *Caenorhabditis elegans*


**Needhi Bhalla[1,2] and Abby F. Dernburg[1,2]***



**We report the discovery of a checkpoint that monitors synapsis between homologous chromosomes to ensure accurate meiotic segregation. Oocytes containing unsynapsed chromosomes selectively undergo apoptosis even if a germline DNA damage checkpoint is inactivated. This culling mechanism is specifically activated by unsynapsed pairing centers, *cis*-acting chromosome sites that are also required to promote synapsis in *Caenorhabditis elegans*. Apoptosis due to synaptic failure also requires the *C. elegans* homolog of *PCH2*, a budding yeast pachytene checkpoint gene, which suggests that this surveillance mechanism is widely conserved.**


Meiosis requires two successive cell divisions: one in which homologous chromosomes separate and a second that partitions sister chromatids. Accurate segregation depends on the establishment of physical linkages (chiasmata) between homologous chromosomes during meiotic prophase. Chromosome pairing, the polymerization of the synaptonemal complex between paired homologs (synapsis), and crossover recombination are all required to generate chiasmata, which enable proper chromosome alignment on the meiotic spindle.

Defects in these early meiotic events can lead to cell cycle arrest or apoptosis, indicating that the events are monitored by checkpoints. In budding yeast, a "pachytene checkpoint" responds to defects in homolog synapsis and/or recombination [reviewed in (*1*)]. Mammalian meiosis may have two distinct checkpoints, one that responds to synaptic failure and one that responds to DNA damage (*2*–*4*). Because synapsis and recombination are obligately coupled in both *Saccharomyces cerevisiae* (*5*) and mice (*3*, *6*), it has been ambiguous whether these checkpoints are triggered by recombination defects or asynapsis. Here, we have exploited the knowledge that synapsis can be complete-


[1]Life Sciences Division, Lawrence Berkeley National Laboratory, [2]Department of Molecular and Cell Biology, University of California, Berkeley, Berkeley, CA 94720, USA.

*To whom correspondence should be addressed. E-mail: afdernburg@lbl.gov